NASA-CR-195159

OPTICAL MATERIALS

Excited state dynamics of thulium ions in Yttrium Aluminum Garnets

G. Armagan, A.M. Buoncristiani
Department of Physics, Christopher Newport College, Newport News, VA 23606, USA

and

B. Di Bartolo
Department of Physics, Boston College, Chestnut Hill, MA 02167, USA

The processes that take place in the excited states of a trivalent Thulium (Tm) ion in an Yttrium Aluminum Garnet (YAG) crystal, being relevant to the use of this system for laser applications, have been the object of several studies. We have reexamined this system, focusing our attention on the dynamics of Tm following its excitation in the $^3H_4$ level. Under these conditions the system relaxes through a cross-relaxation process, $^3H_4 \rightarrow {}^3F_4$, $^3H_6 \rightarrow {}^3F_4$, whose rate depends upon both the concentration of the Tm ion and the temperature of the crystal. The excitation spectrum obtained by monitoring the 1.8 μm emission of Tm (due to the $^3F_4 \rightarrow {}^3H_6$ transition) indicates an increase in the contribution to this emission from the $^3H_4$ level relative to the $^3H_5$ level as the Tm concentration increases; this shows the increased role played by the $^3H_4$ level in pumping the infrared emission. Correspondingly the duration of the luminescence originating in the $^3H_4$ level is shortened as the concentration of Tm increases. The concentration quenching of this lifetime can be fit to a model which assumes that the cross-relaxation is due to a dipole–dipole interaction; from this fit the intrinsic Tm lifetime in absence of cross relaxation can be derived. We have used this lifetime to calculate the rate of the cross-relaxation process. We have evaluated this rate as function of temperature and found it to be fastest at 77 K. We have also calculated the microscopic interaction parameters for the cross-relaxation process by using two independent experimental features: (i) the time evolution of the emission from the $^3H_4$ level, and (ii) the spectral overlap between the $^3H_4 \rightarrow {}^3F_4$ emission and the $^3H_6 \rightarrow {}^3F_4$ absorption. We have also considered the migration of excitation among the Tm ions in the $^3F_4$ level and calculated the relevant microparameter by the use of the relevant spectral overlap. The data are consistent with the model in which the Tm ions, once excited into the $^3H_4$ level decay by cross relaxation to the $^3F_4$ level, and then transfer rapidly their energy to other Tm ions.

1. Introduction

The first detailed studies of the optical properties of solids doped with rare earth ions confirmed that energy transfer among such ions by various resonant inter-ionic interactions was possible: subsequent investigation showed that these processes could even produce luminescence with quantum yields greater than unity [1]. The possibility of using these energy transfer processes to enhance the characteristics of solid state lasers pumped by flash lamps was also recognized early [2]: the sensitization of a laser medium by optically active ions was used to increase the pump efficiency and lower the threshold [3]. Later,

with the emergence of laser-pumped lasers, where the pump radiation populates only one manifold and this excitation finds its way efficiently to lasing levels by one or more transfer process, it became important to understand these energy transfer mechanisms in more detail.

Tm^{3+} in crystalline solids has been used in several important laser applications. The interest in this ion arises mainly from two facts: (i) it has a strong absorption ($^3H_6 \rightarrow {}^3H_4$) in the region where pumping with semiconductor diode lasers can be used [4], and (ii) it efficiently accepts energy transferred from Cr, thus facilitating broadband pumping [5,6]. Tm^{3+} in YAG has been shown to lase [7]: in addition this ion

1

has been used as a sensitizer for Ho [8,9]. A diode-pumped Tm.Ho:YAG laser has been demonstrated by Kintz et al. [10]. Much of this work has indicated the presence of a complex sequence of energy transfer and migration events: these phenomena, being critical to the lasing process either by providing transfer of excitation energy to lasing ions or by producing loss mechanisms, continue to call the attention of workers in the field. A group of researchers at the University of Lyon has conducted a study of such processes involving Tm and Ho in LiYF₄ (YLF) [11]. We are presently conducting a thorough investigation of Cr. Tm and Ho in YAG.

As part of this effort we have investigated the dynamical processes that take place when Cr and Tm are present in a YAG crystal [5,6]. The present work is a logical extension of this previous investigation in that it discusses the processes that take place within the Tm system in YAG, once it has been provided with some excitation energy. In particular, we shall treat the phenomenon of cross relaxation that takes place when the Tm ion is excited to its $^3H_4$ level. This phenomenon has been studied by other workers, some of them using spectroscopic measurements [12], and others laser measurements [13]. We ourselves have dealt with it in the past at various times [14,15]. We shall also address our attention to the energy transfer processes that may take place among Tm ions in their lowest excited $^3F_4$ level. In the present article we would like to present some additional data and, in the process of doing so, treat in a comprehensive way the whole problem of energy transfer in this system.

The most informative work on the spectra and energy levels of Tm³⁺ in YAG is due to Gruber et al. [16], who studied the absorption and emission spectra of this system. The energy level diagram of fig. 1 is merely indicative, in the sense that it reports only the approximate positions of the centroid for each ^{2S+1}L manifold. For greater detail one should look at the work just mentioned.

2. Samples and experimental

Samples of YAG:Tm. grown by the Union Carbide Corporation with various Tm concentrations ranging from 0.75 to 6%, were examined. A typical sample had the dimensions 1.0×1.0×0.5 cm. Some of the
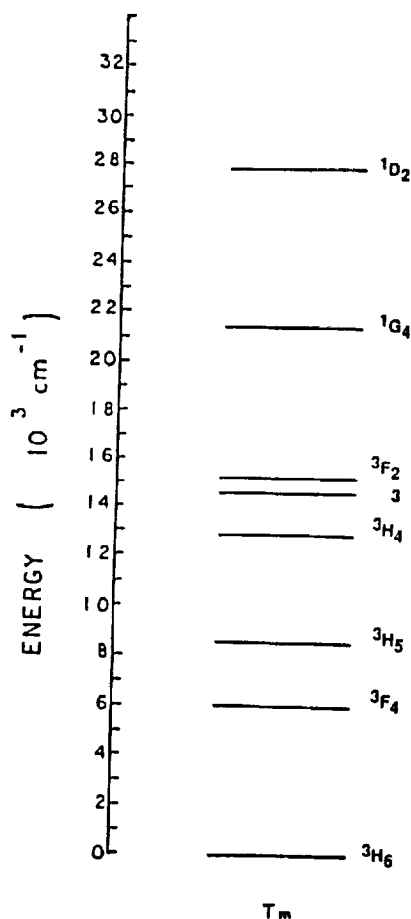

Fig. 1. Energy levels of Tm³⁺ in YAG.

samples were co-doped with Cr, but the presence of the Cr ions was not expected to influence the study of the processes within the Tm system.

The room temperature absorption spectra of the samples were obtained by using a Perkin Elmer Corp. Model Lambda 9 spectrophotometer. The low-temperature absorption spectra were measured in transmission with the same equipment used for the luminescence measurements and described below.

The following sources were available to excite the samples in order to obtain the luminescence spectra: a Jarrell Ash 30W tungsten halogen lamp, a Sharp Corp. Model LTO24MFO diode laser, and a Coherent Inc. Model 526 Ar ion laser. The luminescence was observed at 90 degrees to the direction of excitation, focused onto the entrance slit of a Spex Industries Model 1269, 126 meter scanning monochroma-

tor. The signal in the optical region was detected by a RCA Model C31034 photomultiplier (having a GaAs photocathode, and cooled by a Haake Buchler Instruments, Inc. Model K1 refrigerator), amplified and discriminated by a Spex Industries Model DM 102 Photon Counting Input Module. The signal in the infrared region was detected by a Spex Industries Model 1428 lead sulfide detector and amplified by a Stanford Research Systems Model SR510 lock-in amplifier. Both signals were processed and stored by a Spex Industries Model DM1B spectrometer controller and data processor. Radiation trapping effects were minimized by pumping the samples close to the surface from which luminescence was observed so that the emitted light traveled only a short distance in the sample.

The excitation spectra were obtained by selecting and varying the exciting wavelength by means of a Spex Industries Model 1681, 0.22 m monochromator. The pulsed luminescence measurements were made by using a Quantel International Model TDL-51 tunable dye laser pumped by Quantel International Model 660A-10 Nd:YAG Laser. The length of the pulses produced by these lasers (~10 ns) was much shorter than the decay times measured. The signal detected by either the photomultiplier or a Judson Infrared Inc. Model J12TE2 InAs detector was amplified by an Analogic Data Precision D1000 dual amplifier, processed and stored by an Analogic Data Precision Data 6000 waveform analyzer.

The samples were mounted in either a Janis Research Co., Inc. Model 8DT cryostat or a CTI-Cryogenics Model 12 cold head connected to a Model SC-21 compressor. The sample temperature was varied from 8 to 400 K by using either a Lake Shore Cryotronics Model DRC-80C or a Spectra Physics Model 5720 digital thermometer/controller.

3. Experimental results

3.1. Absorption, luminescence, and excitation spectra

The absorption spectrum of YAG:Tm(1%) obtained at 295 K from 300 to 2600 nm shows bands in correspondence to the transitions from the $^3H_6$ ground level to the $^1D_2$, $^1G_4$, $^3F_2$, $^3F_3$, $^3H_4$, $^3H_5$, and $^3F_4$ levels. Our data are not presented here, on account of

the more complete measurements made by Gruber et al. and reported in ref. [16].

The luminescence spectra of YAG:Tm(1%) in the infrared region at 550, 300 and 78 K are shown in fig. 2; these measurements were made by exciting the sample with a tungsten lamp. The spectral output of this sample includes also a much weaker infrared emission covering the region 1300 to 1550 nm; this emission at room temperature is reported later in this article (in fig. 11).
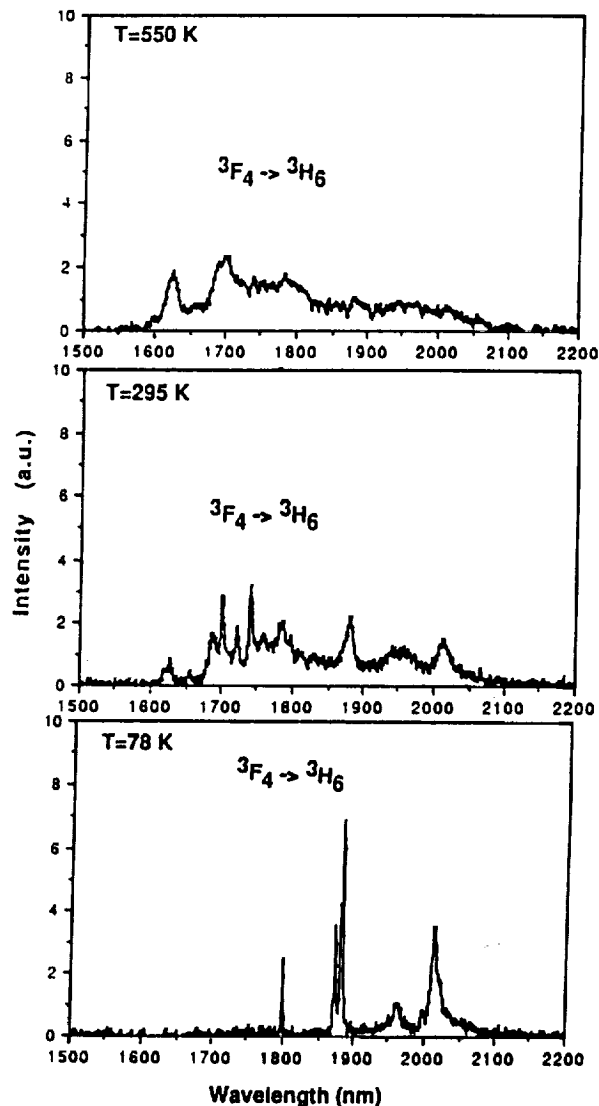

Fig. 2. Infrared luminescence of YAG:Tm (1%) at 78, 295, and 550 K. The region 1.5 to 2.1 μm was covered and a W source was used.

3

In addition, other measurements were run at room temperature by exciting the sample with a tungsten lamp, or by means of an Ar laser. Excitation by the latter at 460 nm resulted in the pumping of level $^1G_4$ and produced evidence of $^1G_4 \rightarrow {}^3H_5$ and $^3H_4 \rightarrow {}^3H_6$ transitions. The study of these additional transitions, not reported in ref. [16], is not relevant to the dynamics of Tm ions following their excitation to the $^3H_4$ level and will be pursued and reported later.

The room temperature excitation spectra obtained by monitoring the emission from the $^3F_4$ manifold for two samples: YAG:Tm(0.75%) and YAG:Tm(6%) are shown in fig. 3. We note the increase in intensity of the peaks corresponding to the $^3F_2$, $^3F_3$ and $^3H_4$ levels relative to the peak corresponding to the $^3H_5$ level, with increasing Tm concentration. This is a clear indication of the increased transfer of excitation within the Tm system, from the $^3H_4$ to the $^3F_4$ manifolds.

3.2. Response to pulsed excitation

The decay curves of the Tm emission from the $^3H_4$ level at room temperature and for several Tm concentrations are shown in fig. 4. For the lowest Tm concentration (0.75%) the decay pattern is exponential, except at very early times ($t < 50$ μs). As the Tm concentration increases the curves assume the shapes generally associated with the decay of a sensitizer in the presence of an increasing number of activators; these curves are very similar to the ones obtained by Becker et al. [17].

If we scale all of the curves so that they have an amplitude 1 at $t = 0$, then the area under an individual curve gives a measure of the duration of that particular decay. We call the value of this area the "lifetime" of the $^3H_4$ level; the variation of this lifetime with Tm concentration is reported in fig. 5.

We have also measured the temperature dependence of the lifetimes as defined above. Fig. 6 shows typical decay curves at 300 and 77 K, for the samples with 2% and 6% Tm concentrations. The results for all the samples examined in the 8 to 350 K range are shown in fig. 7. For the 0.75% Tm concentration the lifetime is almost constant with temperature. For higher Tm concentrations the lifetimes decreases from 8 to 77 K, then starts to increase, and above 200 K remains practically constant. This behavior results in
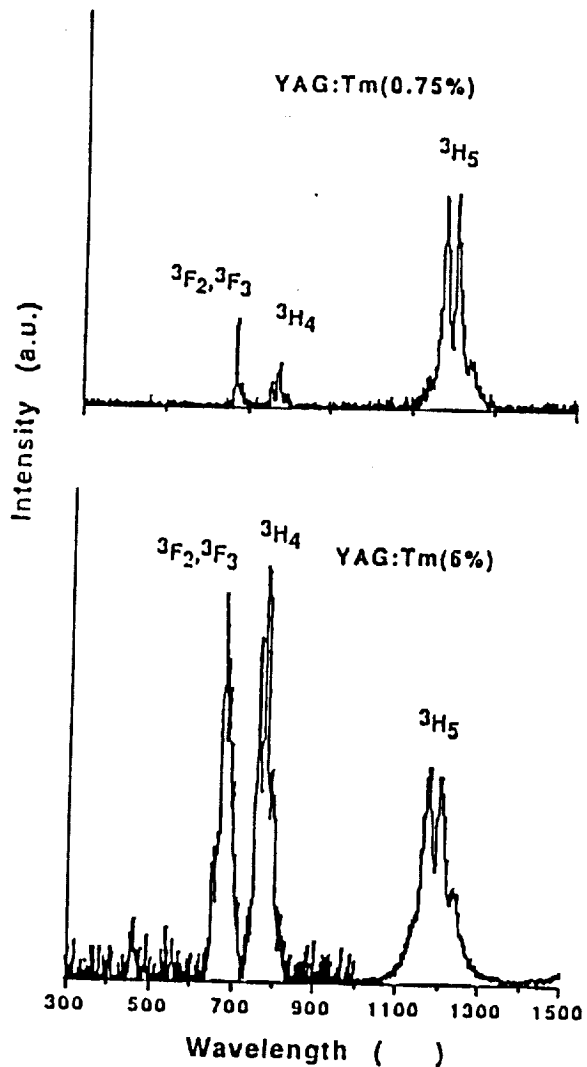
4

Fig. 3. Excitation spectra of YAG:Tm (0.75%) and YAG: Tm (1%) (obtained by monitoring the 1.8 μm emission at room temperature).

a "dip" at 77 K which becomes more evident at the higher Tm concentrations.

The decay curves of Tm emission from the $^3F_4$ level represents a rise due to the filling of this level and a long decay. Lifetime of this decay for Tm (6%) sample shown in fig. 8 decreases as temperature varies from 30 to 295 K.
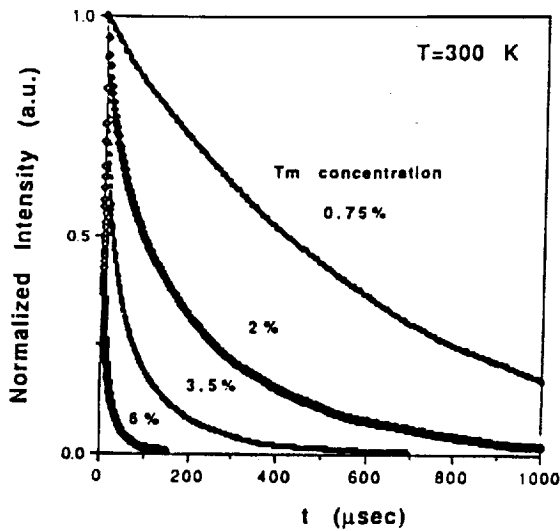
Fig. 4. Decay patterns of the $^3H_4 \to {}^3H_6$ emission ($\lambda=830$ nm) for (1) 0.75%, (2) 2%, (3) 3.5%, and (4) 6% Tm concentrations at room temperature The exciting pulses (at $\lambda=785.5$ nm) were provided by a dye laser.
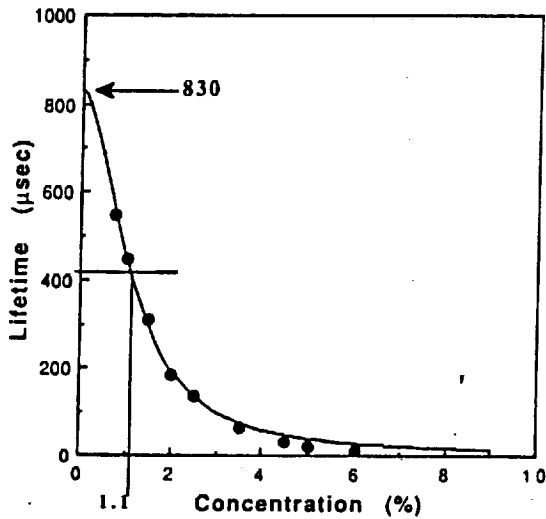

Fig. 5. Lifetimes of the $^3H_4$ level of Tm in YAG as function of Tm concentration at room temperature.

4. Interpretation of results

4.1. The process of cross-relaxation

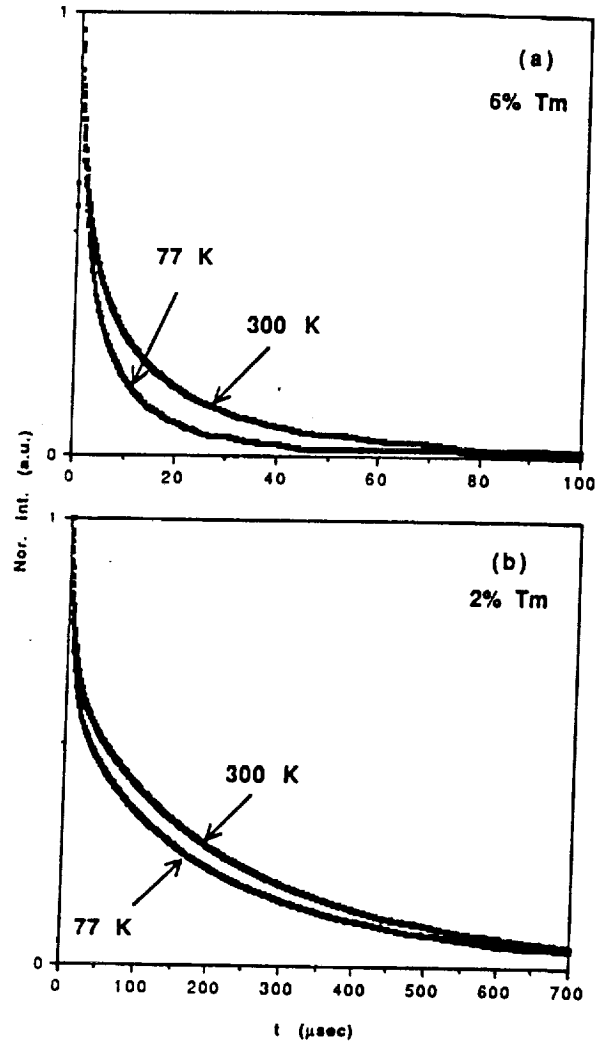Cross-relaxation is an interesting case of energy transfer among ions in solids. Since the ions involved

Fig. 6. Decay pattern of the $^3H_4 \to {}^3H_6$ emission ($\lambda=830$ nm) for (a) 6%, and (b) 2% Tm concentrations at 300 and 77 K. The exciting pulses (at $\lambda=785.5$ nm) were provided by a dye laser.

are of the same type, it presents features that are different than those of the case of energy transfer among different ions. The knowledge derived from such studies is relevant to the laser performance of the Tm ion, by itself or in combination with ions of different types.

The evidence for the existence of a cross-relaxation process $^3H_4 \to {}^3F_4$, $^3H_6 \to {}^3F_4$ is based on a number of experimental results.

Let us consider first the excitation spectra in fig. 3. The excitation spectrum obtained by monitoring the
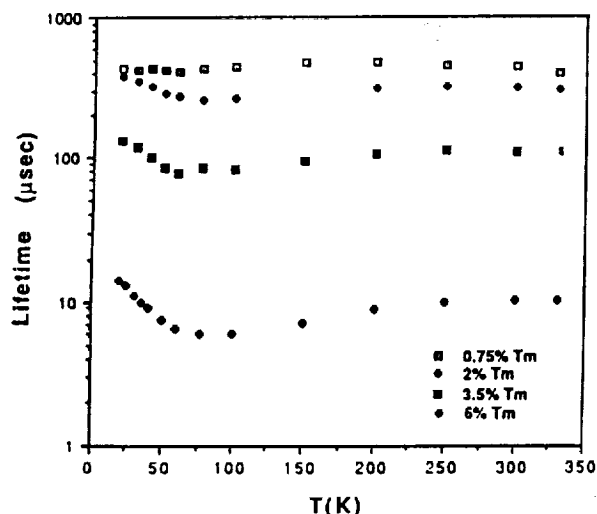
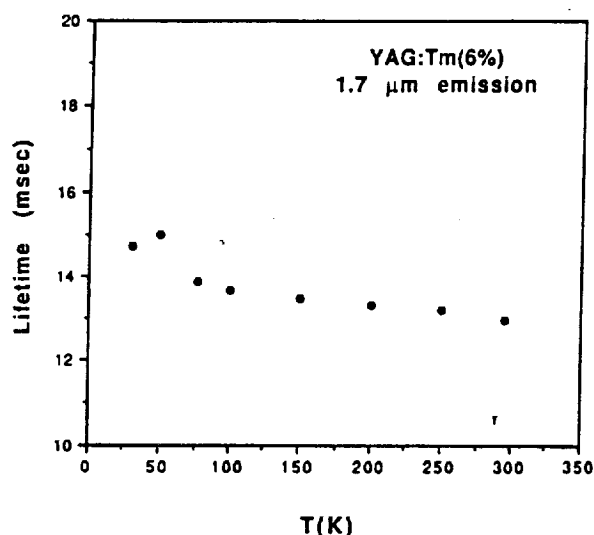Fig. 7. Lifetimes of the $^3H_4$ level of Tm in YAG as function of temperature for several Tm concentrations.

Fig. 8. Lifetimes of the $^3F_4$ level of Tm (6%) in YAG as function of temperature.

1.8 µm emission of Tm (due to the $^3F_4 \rightarrow {}^3H_6$ transition) shows that the emission from the $^3F_4$ level is present when the system is pumped in the $^3F_2$, $^3F_3$, $^3H_4$, and $^3H_5$ levels. The data show also that, as the concentration of Tm increases, the level $^3H_4$, and the levels $^3F_2$ and $^3F_3$, which are connected to it by fast nonradiative processes, are more and more effective than the level $^3H_5$ in pumping the $^3F_4$ level, as one

would expect in the presence of the cross-relaxation process.

The lifetime data provide additional evidence. The lifetime of the luminescence originating in the $^3H_4$ level is quenched as the concentration of Tm increase, confirming that the cross-relaxation path is available to the Tm ion in the $^3H_4$ level. If the interaction between the Tm ions responsible for the cross relaxation is of dipole–dipole type, then the lifetime will depend quadratically on the concentration as follows [19]

$$\tau = \tau_0/[1 + (C/C_0)^2] . \tag{1}$$

In this expression, τ_0 is the intrinsic lifetime of Tm, that is, the lifetime of an isolated Tm ion, in the absence of any cross-relaxation; τ is the lifetime of a Tm ion in a sample with Tm concentration C and it is due both to intrinsic relaxation and cross-relaxation processes; C_0 is the value of the Tm concentration at which the lifetime is reduced by half. Fig. 5 shows the dependence of Tm lifetime on concentration, with the solid curve being the best fit of the data to eq. (1). The intrinsic lifetime of this level determined by extrapolation of the fitted curve to zero concentration is 830 µs; we used this value to calculate the Tm–Tm cross-relaxation rate, p, with the following equation:

$$p = (\tau^{-1} - t_0^{-1})^{-1} . \tag{2}$$

The cross-relaxation rate from the $^3H_4$ level of Tm at room temperature as function of the square of Tm concentration is shown in fig. 9.

We derived the temperature dependence of the cross-relaxation by using the formula (2) and the data on the lifetime of the $^3H_4$ level at different temperatures, assuming that the intrinsic lifetime τ_0 is constant at all temperatures. The results are shown in fig. 10. The rate of the cross-relaxation process is found to increase with increasing Tm concentration at a given temperature; on the other hand, for a certain Tm concentration it presents a maximum at ≈ 77 K.

This temperature dependence is due to the changes of the overlap integral between the $^3H_4 \rightarrow {}^3F_4$ emission and the $^3H_6 \rightarrow {}^3F_4$ absorption; this changes are due to the rearrangements of populations in the $^3H_4$ and $^3H_6$ manifolds. Of course no general conclusion regarding the cross relaxation of Tm ions should be drawn from this finding, which depends on the details of the energy level scheme: as matter of fact, in
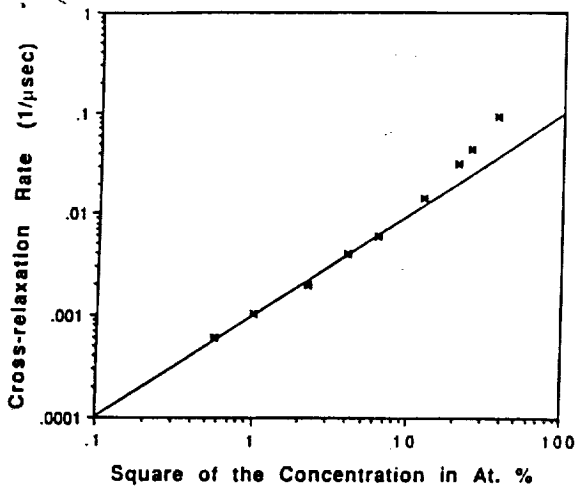
Fig. 9. Cross-relaxation rate among Tm ions in YAG as a function of the square of the Tm concentration at room temperature.

a similar study of ours of cross relaxation of Tm ions in the host lattice LiYF$_4$, we have found a cross-relaxation rate decreasing with temperature with no maximum in the curve of rate versus temperature [20].

4.2. Microparameter for cross relaxation

The rate of the energy transfer between a sensitizer ion (S) and an activator ion (A), w_{SA}, depends on

the separation between the ions. R. This dependence can be expressed in a multipolar expansion as follows:

$$w_{SA}(R) = C^{(6)}/R^6 + C^{(8)}/R^8 + C^{(10)}/R^{10} + \dots ,$$

$$(3)$$

where the first three terms corresponds to dipole–dipole, dipole–quadrupole, and quadrupole–quadrupole interactions, respectively. If there is a dominant multipolar interaction, then the transfer rate assumes the simpler form

$$w_{SA}(R) = C^{(n)}/R^n ,$$

$$(4)$$

and we can define an "energy transfer" radius, R_0, as follows:

$$w_{SA}(R) = C^{(n)}/R^n = \tau_0^{-1}(R_0/R)^n ,$$

$$(5)$$

where τ_0 is the effective decay time of S in absence of A and R_0 is the separation between ions at which the energy transfer rate is equal to the decay rate of sensitizer.

The characteristic energy transfer radius R_0 in the case of dipole–dipole interaction R_0 is given by [1]

$$R_0^6 = \epsilon(3e^2/mc^2 2^6\pi^4)f_A \int \lambda^6 g_S(\lambda) g_A(\lambda) \, d\lambda .$$

$$(7)$$

In this expression, ϵ is the quantum efficiency of the donor luminescence (in the absence of any acceptor), that is

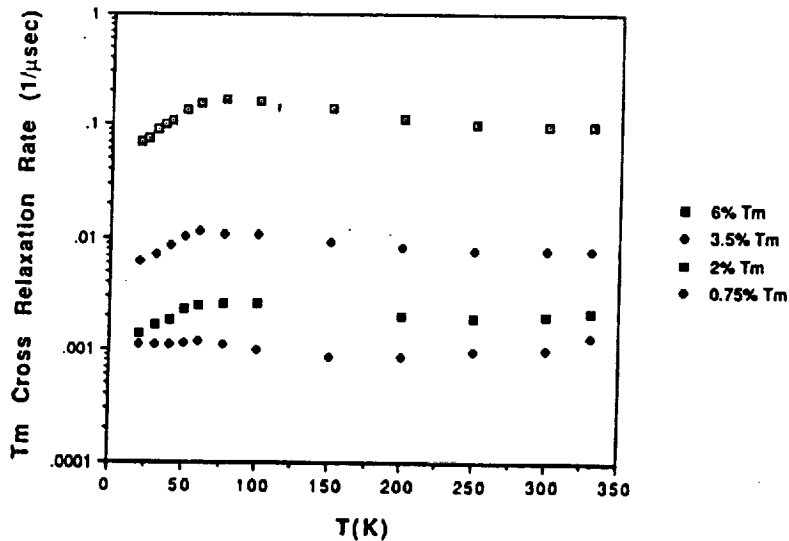
Fig. 10. Cross-relaxation rate among Tm ions in YAG as a function of temperature for several Tm concentrations.

7

$$\epsilon = (\text{probability of radiative decay})$$

$$\times (\text{probability of radiative decay}$$

$$+ \text{probability of nonradiative decay})^{-1}. \qquad (6)$$

The overlap integral involves $g_S(\lambda)$ and $g_A(\lambda)$, the normalized emission and absorption data as

$$f_A = (mc^2 n/\pi e^2 c_A) \int (1/\lambda^2) \, \alpha_t(\lambda) \, d\lambda. \qquad (8)$$

Here n is the index of refraction. c_A and $\alpha_A(\lambda)$ are the concentration and the absorption coefficient of the activator, respectively.

The microscopic interaction parameter of eq. (4), given by

$$C^{(6)} = R_0^6/\tau_0, \qquad (9)$$

is the probability per unit time of energy transfer when S and A are at the distance of 1 cm. We have calculated this parameter for the $^3H_4 \rightarrow \, ^3F_4$, $^3H_6 \rightarrow \, ^3F_4$ cross-relaxation process using the approximation that the concentration of activator ions, c_A, is the total concentration of Tm ions.

The spectral data relevant to this calculation are the normalized Tm emission corresponding to the $^3H_4 \rightarrow \, ^3H_4$ transition and the normalized Tm absorption corresponding to the $^3H_6 \rightarrow \, ^3F_4$ transition. These data at room temperature are shown in fig. 11. The various quantities entering the expression for and the value of the microparameter are reported in table 1. The quantity ϵ was calculated taking the ratio of the lifetime at room temperature to the lifetime at 30 K.

The time evolution of the emission from a sensitizer's level following a pulsed excitation may provide an additional and independent way of finding a value for the energy transfer microparameter. This is certainly so when no fast diffusion among sensitizers is present. In such a case the decay of the sensitizer is expressed by the following expression [21]:

$$p(t) = \exp[-t/\tau_0$$

$$-c_A/(4\pi R_0^3/3) \, \Gamma(1-3/n) \, (t/\tau_0)3/n]. \qquad (10)$$

where n is either 6 (dipole–dipole). 8 (dipole–quadrupole) or 10 (quadrupole–quadrupole). We can definitely apply this formula to the present case of cross relaxation because, as we shall discuss in the following section 4.3. the migration of excitation en-

ergy among the Tm ions in level $^3H_4$ is slow compared to cross relaxation [17].

Indeed we have been able to reproduce the curves which appear in fig. 4 by using eq. (10) in which we have substituted the intrinsic lifetime of the $^3H_4$ level (830 μs) and values of R_0 close to the one given by the previous calculation and appearing in table 1. We used the value given in this table. 11 Å. to fit the decay curve corresponding to the 3.5% concentration, and we used the values 8. 10. 13 for the curves corresponding to 0.75. 2. and 6%. respectively. The curves that we have generated are reported in fig. 12 and are very close to the experimental curves of fig. 4.

4.3. Energy migration among Tm ions in the level $^3H_4$

When the Tm ions are excited to the level $^3H_4$, in addition to the cross-relaxation process. a process of migration of the excitation energy among Tm ions can in principle take place. How fast is this process in comparison to the cross relaxation? We expect this latter process to be faster for the following reason.

If the migration were very fast the excited Tm ions, being strongly coupled to each other, would form a system with a single decay pattern. The decay curves (see fig. 4). instead. obey eq. (10). This formula applies to systems with various sensitizers in the crystal having various rates of decay which combine in giving the expression (10). We note also that the rate of this migration has been measured by other workers and found to be much slower than the cross-relaxation rate [17].

4.4. Energy migration among Tm ions in the level $^3F_4$

Migration can also take place when the Tm ions are residing in level $^3F_4$, following the process of cross relaxation. The decay curves of this emission indicates two main features: a rise due to the cross relaxation and an exponential decay. The lifetime of this decay for Tm (6%) sample as function of temperature is reported in fig. 8. We have calculated the microscopic interaction parameter for the related energy transfer process $^3F_4 \rightarrow \, ^3H_6$. $^3H_6 \rightarrow \, ^3F_4$ by using Dexter theory [1].
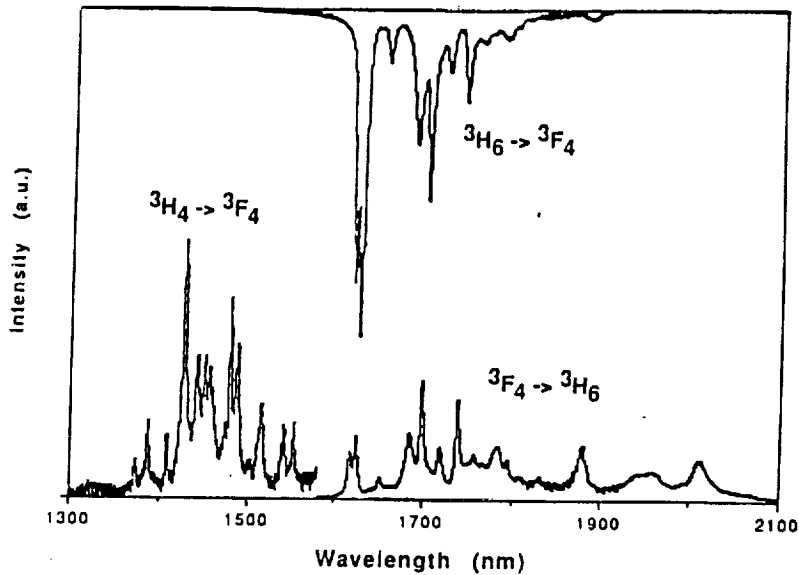
8

Fig. 11. Spectral data used to calculate the overlap integrals relevant to the cross relaxation and migration processes at room temperature.

Table I
Microparameters of Tm:YAG at room temperature for (a) cross relaxation ($^3H_4 \to {}^1F_4$; $^3H_6 \to {}^1F_4$) and (b) migration (among $^3F_4$) processes.

	$c_\tau^{-1} \int \lambda^{-2} \alpha(\lambda) \, d\lambda$ (cm)	$\int \lambda^6 g_S(\lambda) g_A(\lambda) \, d\lambda$ (cm³)	ϵ	R_0 (Å)	$C^{(6)}$ (cm⁶/s)
(a)	1.29×10^{-18}	0.62×10^{-20}	0.83/0.83	11.4	0.27×10^{-38}
(b)	1.29×10^{-18}	75×10^{-20}	13/15	25	1.7×10^{-38}

$(3n/2^6\pi^5 = 2.7 \times 10^{-4})$

The spectral data relevant to this calculation are the normalized Tm emission corresponding to the $^3F_4 \to {}^3H_6$ transition and the normalized Tm absorption corresponding to the $^3H_6 \to {}^3F_4$ transition. These data at room temperature are shown in fig. 11. The various quantities entering the expression for and the value of the microparameter are reported in table I.

French and Powell have used laser-induced grating spectroscopy to measure spatial energy migration *without* spectral transfer [22] by using the four-wave mixing technique. They report data from which we can derive a value for R_0 of ~100 Å: this value is expected to be larger than the one derived by using the Dexter theory [1,23] and dealing with partial overlap.

5. Conclusions

On the basis of our experimental observations and of our related calculations we can present the following conclusions:

(i) We have found additional evidence that supports the model proposed by other workers for the dynamics of Tm ions following their excitation to the $^3H_4$ level (see, for example, ref. [4]). According to this model, excitation of an ion to this level is followed by a fast cross-relaxation process whose rate increases with concentration and is temperature dependent with a maximum value at 77 K.

(ii) Another inter-ionic process may transfer the excitation of a particular ion in the $^3H_4$ level to a different Tm ion, thus producing a migration of the excitation energy. This process is much slower than the cross-relaxation process.
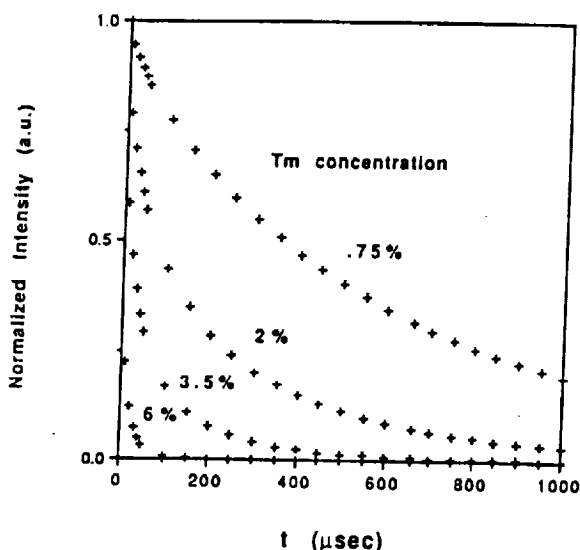
9

Fig. 12. Curves of sensitizer ($^3H_4$) decay obtained by using formula (10).

(iii) Following the cross relaxation of a Tm ion to the $^3F_4$ level a migration of this excitation sets in. The rate of such process is found to be greater than that of cross relaxation and, because of it, the excitation energy diffuses easily among the Tm ions, a very useful condition if, as it may be the case, Tm is used to sensitize other ions, such as Ho. We note here that the result obtained by other workers [23] and by us [24] indicate that, for the usual condition used in laser applications of much larger Tm than Ho concentration, the migration of the $^3F_4$ excitation energy is faster than the energy transfer between Tm and Ho ions.

(iv) We have measured the microparameter associated with the cross relaxation process and the microparameter associated with the migration of $^3F_4$ excitation energy. In particular the former has been obtained by using two different kind of data: the spectral data and the details of the kinetics of the cross relaxing level. The latter has been obtained by using solely spectral data. We trust that, besides providing additional evidence for the existing model, we have put it on a more quantitative basis.

Acknowledgements

References

[1] D.L. Dexter, J. Chem. Phys. 212 (1953) 836, Phys. Rev. 108 (1957) 630.

[2] A.A. Kaminskii, Laser crystals, their physics and properties (Springer, Berlin, 1981, 1990).

[3] L.F. Johnson, J.E. Geusic and L.G. Van Uitert, Appl. Phys. Lett. 8 (1966) 200.

[4] T.Y. Fan, G. Huber, R.L. Byer and P Mitzscherlich, IEEE J. Quantum Electronics 24 (1988) 924.

[5] G. Armagan, B. Di Bartolo and A.M. Buoncristiani, J. Luminescence 44 (1989) 129.

[6] G. Armagan, B. Di Bartolo and A.M. Buoncristiani, J. Luminescence 44 (1989) 141.

[7] L.F. Johnson, J.E. Geusic and L.G. van Uitert, Appl. Phys. Lett. 7 (1965) 127.

[8] B.M. Antipenko, A.S. Glebov, T.I. Kiseleva and V.A. Pismennyi, Opt. Spectr. (USSR) 63 (1987) 230.

[9] J.K. Tyminsky, D.M. Franich and M. Kokta, J. Appl. Phys. 65 (1989) 15.

[10] G.J. Kintz, L. Esterowitz and R. Allen, Electron. Lett. 23 (1987) 616.

[11] A. Brenier, J. Rubin, R. Moncorgé and C. Pedrini, J. Phys. (France) 50 (1989) 1463.

[12] B.M. Antipenko, A.S. Glebov, T.I. Kiseleva and V.A. Pismennyi, Opt. Spectr. (USSR) 60 (1986) 95.

[13] G.J. Kintz, R. Allen, and L. Esterowitz, Postdeadline Papers, Conf. Laser Electro-Opt. (Optical Society America, Washington DC 1987).

[14] G. Armagan, A.M. Buoncristiani, W.C. Edwards, A.T. Inge and B. Di Bartolo, OSA Proc. on Advanced solid state lasers, Vol. 6, eds. H.P. Jenssen and G. Dubé (Optical Society of America, Washington DC 20036, 1990) p. 144.

[15] G. Armagan, A.M. Buoncristiani and B. Di Bartolo, J. Luminescence 48&49 (1991) 171.

[16] J.B. Gruber, M.E. Hills, R. Macfarlane, C.E. Morrison, G.A. Turner, G.J. Quarles, G.J. Kintz and L. Esterowitz, Phys. Rev. B 40 (1989) 9464.

[17] T. Becker, R. Clausen, G. Huber, E. Duczynski and P. Mitzscherlich, OSA Proc. on Advanced solid state lasers, Vol. 5 eds. M.L. Shand and H.P. Jenssen (Optical Society of America, Washington, DC 20036, 1989) p. 154.

[18] D.L. Dexter and J.H. Schulman, J. Chem. Phys. 22 (1954) 1063.

[19] G. Armagan, M. Buoncristiani, A.T. Inge and B. Di Bartolo, Advanced Solid State Laser Conf., Hilton Head, S.C., March, 1991, paper TuC3-1.

[20] M. Inokuti and F. Hirayama, J. Chem. Phys. 43 (1963) 1978.

[21] V.A. French and R.C. Powell, Optics Lett. 16 (1991) 666.

[22] R.C. Powell, private communication.

[23] G. Armagan, M. Buoncristiani and B. Di Bartolo, to be published.